HEFAT2012
9th International Conference on Heat Transfer, Fluid Mechanics and Thermodynamics
16 – 18 July 2012
Malta

THERMO-FLOW CHARACTERISTICS OF A PIN-FIN RADIAL HEAT SINKS ACCORDING TO THEIR FIN HEIGHT PROFILE

Daeseok Jang and Kwan-Soo Lee*
*Author for correspondence
School of Mechanical Engineering,
Hanyang University,
222 Wangsimni-ro, Seongdong-gu, Seoul, 133-791,
Korea,
E-mail: ksleehy@hanyang.ac.kr

ABSTRACT

In this study, the thermo-flow characteristics of pin-fin radial heat sinks were investigated according to their fin height profile. A pin-fin radial heat sink is composed of a horizontal circular base and rectangular pin fins. Pin-fin radial heat sinks with differing fin height profiles were examined so that one could be designed for large-output light-emitting diode (LED) products using the same heat sink mass as reported for previous plate-fin heat sinks. Both natural convection and radiation heat transfer were considered in the investigation. The thermal resistances of heat sinks with various types of pin-fin arrays were compared to determine an appropriate reference configuration. A parametric study was then performed to compare the effects of five geometric parameters (outermost fin height, difference between fin heights, number of fin arrays, long fin length, and middle fin length) on thermal resistance. The effects of the outermost fin height and the number of fin arrays were found to be significant.

INTRODUCTION

The market for light-emitting diode (LED) lighting systems has recently been expanding since LED lights have longer lifespans than conventional lights, as well as higher energy efficiency. Almost a 30% reduction in power consumption can be realized by switching from conventional to LED lighting. If the lighting is controlled systematically, a further 30% reduction is possible due to the fact that LED lighting can be controlled by a single unit and a central controller that responds to environmental changes, leading to maximized energy savings. The market share of LED lighting is growing rapidly on the strength of its high energy efficiency, and the market domain now includes large-output LED products. Optimization of radial heat sinks, a cooling apparatus for LED lighting applications, is necessary to obtain reliable cooling performance in large-output LED products.

NOMENCLATURE

A	[mm^2]	surface area for heat transfer
C_p	[J/(kg·K)]	specific heat
F	[-]	view factor
H	[mm]	fin height
h	[W/(m^2·K)]	heat transfer coefficient
I	[W/m^2·sr]	Intensity of radiation
k	[W/(m·K)]	thermal conductivity
L	[mm]	length
M	[kg]	Mass of heat sink
N	[-]	Number
n		Normal direction vector
P	[Pa]	pressure
$\dot{q}$	[W/m^2]	Heat flux
$\dot{Q}$	[W]	Heat transfer rate
R_{TH}	[^{o}C/W]	thermal resistance
r	[mm]	radius
$\vec{s}$		Ray direction vector
T	[K]	Temperature
t	[mm]	Thickness of fin
V	[mm^3]	Volume
$\mathbf{v}$	[m/s]	Velocity vector

Subscripts

A	Array
a	air
avg	average
D	Difference between fin heights
f	fin
L	Long fin
M	Middle fin
O	Outermost fin height
s	Space between fins along radial direction
w	wall
∞	ambient

There have been a number of recent studies of radial heat sinks. Yu et al. [1] studied plate-fin radial heat sinks by modeling natural convection, and proposed a correlation to predict the Nusselt number. Yu et al. [2] compared various fin arrays, and found that geometries with long and middle (LM) fins provided the best cooling performance. Multi-objective optimization was carried out to investigate cooling performance and mass simultaneously, using the LM type as a reference case. Yu et al. [3] analyzed the effects of design parameters on radiation heat transfer in radial heat sinks, and optimized the fin configuration. They discovered that when the number of fins, long fin length, and middle fin length were considered simultaneously, the effect of radiation on the total heat transfer was greater than the effect of natural convection, due to interactions. Jang et al. [4] examined radial heat sinks with pin fins to obtain a lighter heat sink with a cooling performance similar to that of a plate-fin heat sink investigated in previous studies [1–3]. In this way, they were able to reduce the mass by more than 30% while maintaining a cooling performance similar to that of the plate-fin heat sink. However, since these studies were based on the assumption of uniform fin height, their results are unsuitable for radial heat sinks with chimney flow characteristics.

Several recent studies have focused on the behavior of heat sinks in terms of fin height profile. Yang and Peng [5] conducted a numerical study of pin-fin heat sinks with non-uniform fin heights, and concluded that the junction temperature can be reduced by increasing the pin height near the center of the heat sink. Furthermore, the potential exists for optimizing non-uniform fin height designs. Bello-Ochende et al. [6] optimized a pin-fin heat sink design to maximize forced convection with limited mass, and obtained what appeared to be maximum cooling performance when the fin diameter and height were non-uniform. However, these studies were concerned with heat sinks with rectangular bases. Research on radial heat sinks in terms of fin height profile is still lacking.

In the present study, the thermo-flow characteristics of pin-fin radial heat sinks are investigated according to fin height profile. The numerical model used in this study includes both natural convection and radiation heat transfer. Various fin height profiles are compared to determine a reference configuration for a parametric study. The parametric study is then performed to compare the effects of five geometric parameters (outermost fin height, difference between fin heights, number of fin arrays, long fin length, and middle fin length) and determine the sensitive variables for thermal resistance.

MATHEMATICAL MODELING

Numerical model

Figure 1 illustrates a radial heat sink composed of a circular base and pin fins. The fins are radially arranged at regular intervals. The heat-sink base is positioned horizontally, while the fins are attached vertically. The arrangement of the fins is repeated along the circumference of the heat-sink base. Considering the required computational time and number of grids, only a single set of fins (Figure 2) was selected for a computational domain, and these were defined as a single-fin array. The following assumptions were imposed for the numerical analysis.

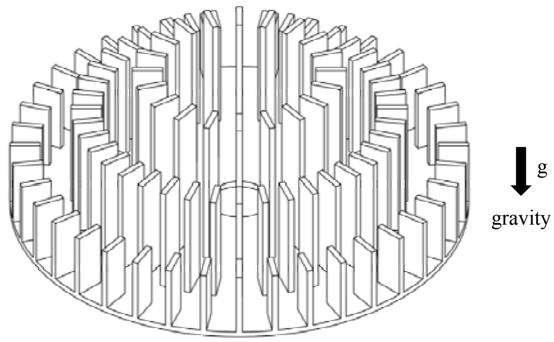

Figure 1 Geometry of a radial heat sink with pin fins

(1)The flow is three-dimensional, steady, and laminar.

(2)The density of air can be calculated using the ideal gas law.

(3)The fluid properties are constant except for the density of air.

(4)The surface of the heat sink is diffuse and gray.

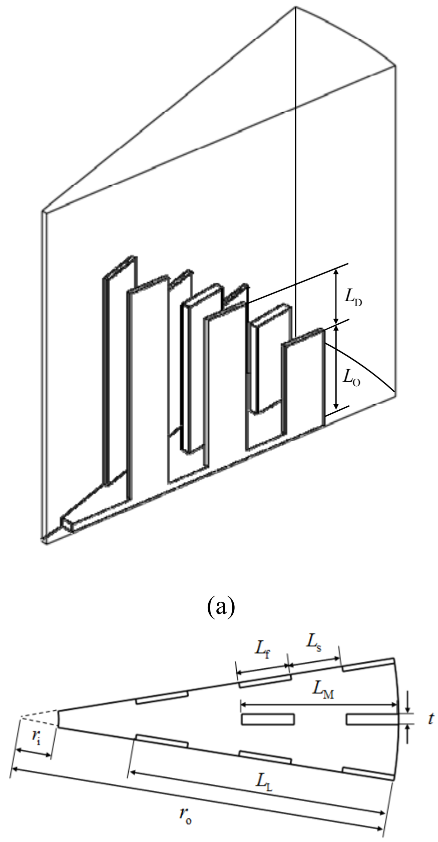

(b)

Figure 2 (a) Isometric and
(b) top view of the computational domain

Governing equations

The governing equations are as follows.

Air side

Continuity equation

$$\nabla \cdot (\rho \mathbf{v}) = 0 \qquad (1)$$

Momentum equation

$$\rho \frac{D\mathbf{v}}{Dt} = -\nabla P + \mu \nabla^2 \mathbf{v} + \mathbf{F} \qquad (2)$$

(for z-direction $\mathbf{F} = -\rho g$)

Energy equation

$$\rho C_p \frac{DT}{Dt} = \nabla \cdot (k \nabla T) + \frac{DP}{Dt} \qquad (3)$$

Fin side

$$\nabla^2 T = 0 \qquad (4)$$

Radiation heat transfer

Radiation heat transfer is calculated by the Discrete Transfer Radiation Model (DTRM), which supports periodic boundary conditions. The radiation heat transfer at the interface between the heat sink and air is

$$\dot{q}_{\mathrm{in}} = \int_{\vec{s}\cdot\vec{n}>0} I_{\mathrm{in}} \vec{s} \cdot \vec{n} d\Omega \qquad (5)$$

$$\dot{q}_{\mathrm{out}} = (1-\varepsilon_{\mathrm{w}}) q_{\mathrm{in}} + \varepsilon_{\mathrm{w}} \sigma T_{\mathrm{w}}^4 \qquad (6)$$

where Ω is the hemispherical solid angle, I_{in} is the intensity of the incoming ray, $\vec{s}$ is the ray direction vector, and $\vec{n}$ is the normal direction vector. T_{w} is the surface temperature and ε_{w} is the wall emissivity.

Boundary conditions and numerical procedure

The following boundary conditions were applied.
(1) Heat sink base: constant heat flux
(2) Periodic interface (solid): symmetric condition
(3) Periodic interface (fluid): periodic condition
(4) Outer faces of the fluid domain: pressure inlet/outlet condition
(5) Interface between the fluid and solid:

$$T_{\mathrm{a,w}} = T_{\mathrm{f,w}} \ , \quad -k_{\mathrm{a}} \left.\frac{\partial T_{\mathrm{a}}}{\partial n}\right|_{\mathrm{w}} + \dot{q}_{\mathrm{out}} = -k_{\mathrm{f}} \left.\frac{\partial T_{\mathrm{f}}}{\partial n}\right|_{\mathrm{w}} + \dot{q}_{\mathrm{in}} \qquad (7)$$

The numerical analysis was conducted using Fluent V6.3, a commercially available computational fluid dynamics (CFD) code based on the finite volume method. The Semi-Implicit Method for Pressure-Linked Equations (SIMPLE) algorithm was used to couple the velocity and pressure.

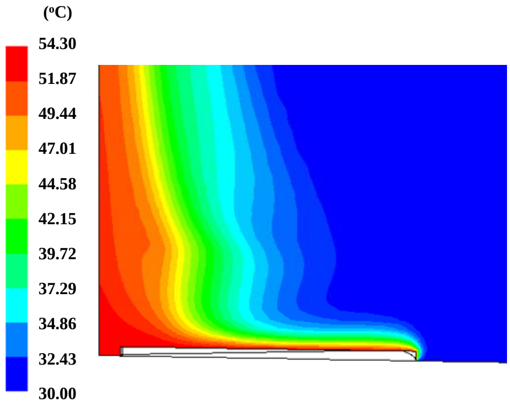

(a) Temperature contours ($\theta = 9°$)

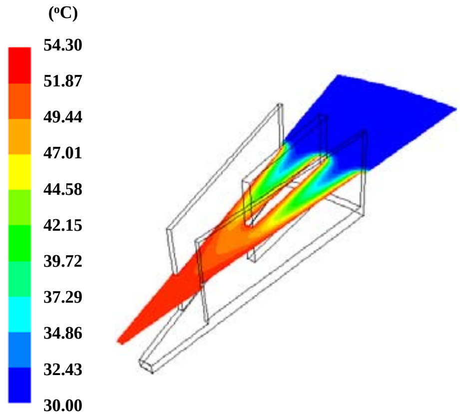

(b) Temperature contours (H=10mm)

Figure 3 Thermo-flow characteristics around a radial heat sink (r_o = 0.075 m, $\dot{q}$ = 700 W/m^2, T_∞ = 30°C)

To improve the accuracy of the analysis, a second-order upwind scheme was applied to the convective terms of the governing equations. The convergence criterion for all dependent variables was a relative error less than 10^{-5}. Denser grids were generated in regions of the domain where a boundary layer developed around the heat sink. To select the computational domain size, the height of the domain was varied from $2H$ to $10H$, and the radius of the domain was varied from $1.3r_o$ to $1.6r_o$. Increasing the height and radius beyond $5H$ and $1.5r_o$, respectively, changed the average heat sink temperature by less than 0.5%. Additionally, the grid dependence was investigated by varying the number of grid points from 60,000 to 700,000. We selected 519,375 grid points as a reference for parametric study; additional grid points produced a change of less than 0.5% for the average heat sink temperature for the reference model.

RESULTS AND DISCUSSION

A heat sink suitable for chimney flow was determined by considering thermo-flow characteristics not only in the horizontal plane, but also in the vertical plane. The plate-fin heat sink proposed by Yu et al. [2] was compared with pin-fin heat sinks with differing fin height profiles by analyzing their cooling performance and mass. Thermo-flow characteristics in both the horizontal and vertical planes were examined by including fin height profile design parameters in the parametric study.

Thermo-flow characteristics around a radial heat sink

Figure 3 shows the temperature contours and velocity vectors around a radial heat sink with an LM plate-fin array (N_A = 20, L_L = 50 mm, L_M = 20 mm, r_o = 75 mm, r_i = 10 mm, H = 21.3 mm, and t = 2 mm, where N_A is the number of fin arrays, L_L is the long fin length, L_M is the middle fin length. The overall flow consists of two components. The vertical flow is upward because the air adjacent to the heat sink is warmed by the higher temperature of the heat sink, and becomes lighter than the surrounding air. The horizontal flow proceeds from the outer region of the heat sink, parallel to the base, and merges with the upward flow of heated air in the inner region. Therefore, the overall flow is composed of relatively cool air entering from the outer region of the heat sink, and rising air in the inner region. This flow pattern is called a chimney flow.

In previous studies of thermo-flow characteristics in a horizontal plane, the number of fin arrays and the fin lengths were design variables for optimization, and are influential design variables in this case. However, it is inappropriate to base the selection of design parameters for a three-dimensional radial heat sink flow on two-dimensional thermo-flow characteristics. In other words, non-uniform heat transfer with respect to the radial direction must be reflected in the design procedure. Comparatively little heat transfer occurs in the inner region because the temperature difference between the air and the heat sink is small. In addition, heated air from the outer region rises above the inner fins in a chimney flow. Therefore, uniform fin height, which was assumed in previous studies, is unsuitable for a non-uniform heat transfer distribution.

Fin height profile

To investigate the three-dimensional flow characteristics of radial heat sinks, the effects of various fin height profiles on the average temperature and mass were examined. The LM plate-fin array was compared to a pin-fin array with the tallest fins on the inside (Type 1) and a pin-fin array with the tallest fins on the outside (Type 2). In general, cooling performance improves with increasing heat sink mass. Accordingly, pin-fin heat sinks with the same mass as the LM plate-fin array were used for the comparison. The parameters of the Type 2 pin-fin array were N_A = 20, L_L = 50 mm, L_M = 30 mm, L_f = 10 mm, L_O = 46 mm, L_D = 15 mm, L_s = 10 mm, r_o = 75 mm, r_i = 10 mm, t = 2 mm, T_{air} = 30°C, $\dot{q}$ = 700 W/m^2, and ε = 0.7, where L_O is the outermost fin height, L_D is the difference between fin heights. For the Type 1 pin-fin array, L_O = 46 mm, and for the LM plate-fin array, N_A = 20, L_L = 50 mm, L_M = 30 mm. Figure 4 shows the temperature contours of the horizontal planes at H = 10 mm for the LM plate-fin array (Yu et al. [2]) and the two fin height profiles considered here. The results of the numerical analysis are listed in Table 1. When the Type 1 height profile was used in place of the LM plate-fin array, the average temperature decreased by 4°C. Repeated leading-edge effects appeared because the fins were arranged to maintain the flow at a certain distance in the radial direction. In addition, a thermal boundary layer developed discontinuously, and its development was delayed. Thus, there was a relatively high temperature difference between the air and the heat sink in the inner regions. At the same time, heat transfer occurred between heated air from the outermost fins and the second row of fins in the chimney flow path. This moving air was not sufficiently heated at the outermost fins to fully develop a thermal boundary layer. Hence, a relatively high local heat transfer

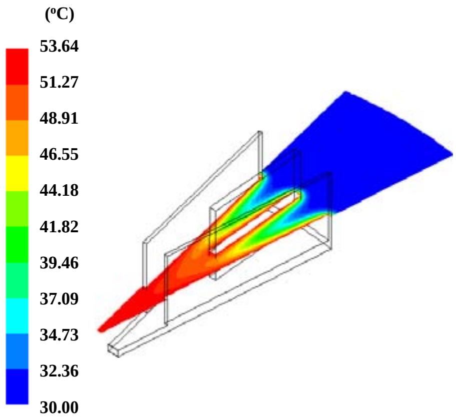

(a) LM model

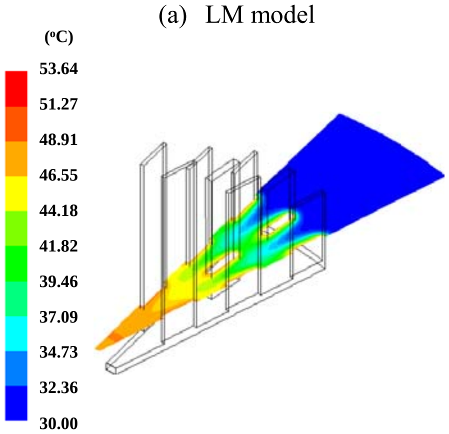

(b) Type 1 height profile

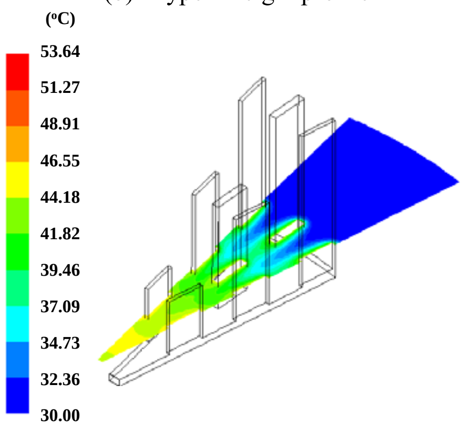

(c) Type 2 height profile

Figure 4 Temperature contours at H = 10 mm (r_o = 0.075 m, $\dot{q}$ = 700 W/m^2, T_∞ = 30°C)

Table 1 Comparison of various fin height profiles

Model	A [mm^2]	L_O [mm]	L_D [mm]	T_{avg} [°C]	Mass [kg]	$\dot{m}$ [10^{-5} kg/s]
LM Type	4499	21.3	0	53.12	0.288	3.04
Type 1	5000	22	15	48.86	0.288	4.39
Type 2	5000	46	15	44.80	0.288	6.4

coefficient appeared on the upper sections of the fins in the second row. In addition, a certain amount of inflow reached the second row of fins, since they were taller than the outermost fins. Such flow characteristics were repeated along the radial direction, and the mass flow rate increased by 44% compared to the LM model. Thus, the cooling performance improved, even though the mass of the Type 1 height profile was same as that of the LM model.

When the Type 2 height profile was used in place of the LM plate-fin array, the average temperature decreased by 8.3°C. The ratio of the outermost fin area to the total fin area was increased by 90%, and the mass flow rate increased by 46% compared to the Type 1 height profile. Since the heat capacity increased with the mass flow rate, the cooling performance was improved. Although the Type 1 height profile exhibited repeated heat transfer along the chimney flow path, the mass flow rate increment of the Type 2 height profile had a greater influence on the cooling performance.

Parametric study

The effects of L_O, L_D, N_A, L_L, and L_M on the thermal resistance were analyzed. The values of the parameters for the reference model were L_O = 50 mm, L_D = 3 mm, N_A = 20, L_L = 34 mm, L_M = 14 mm, L_f = 2 mm, L_s = 2 mm, r_o = 75 mm, r_i = 10 mm, t = 2 mm, T_{air} = 30°C, and $\dot{q}$ = 700 W/m^2. The one-factor-at-a-time method (OFAT), which sorts influential parameters by analyzing the main effect of each, was selected for the sensitivity analysis. The parametric study was conducted by varying L_O, L_D, N_A, L_L, and L_M using four levels for each.

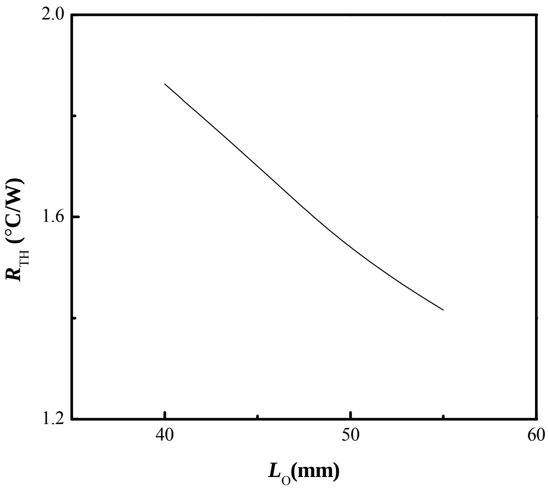

Figure 5 Effect of outermost fin height

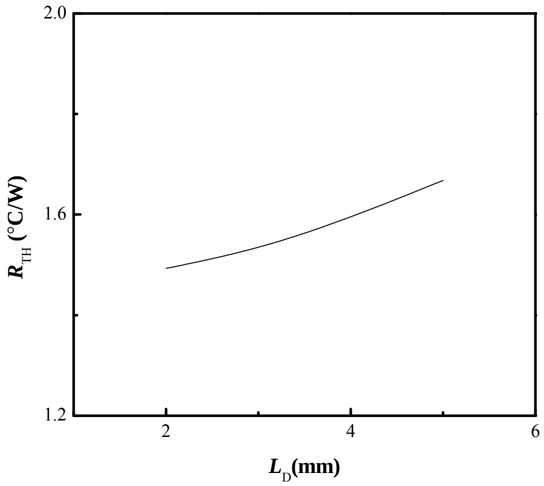

Figure 6 Effect of the difference between fin heights

Figure 5 shows the effect of the outermost fin height (L_O). As L_O increased, the mass flow rate also increased owing to the larger heat transfer area in contact with the cooling air. Thus, the heat capacity of the cooling air increased, and consequently, the thermal resistance decreased.

Figure 6 shows the effect of the difference between fin heights (L_D). As L_D increased, the thermal resistance also increased because the heat transfer area of the inner region decreased for a constant outermost fin height. However, the effect of this parameter on the thermal resistance was not significant, since the outermost fin height, which is the effective parameter for mass flow rate, was fixed.

Figure 7 shows the effect of the number of fin arrays (N_A) on the thermal resistance. As N_A increased, the thermal resistance exhibited a decreasing tendency. The tendency was different from the effect of the number of fin arrays for the LM plate-fin array and the pin-fin model with uniform fin height because the mass flow rate was doubled by using the Type 2 height profile.

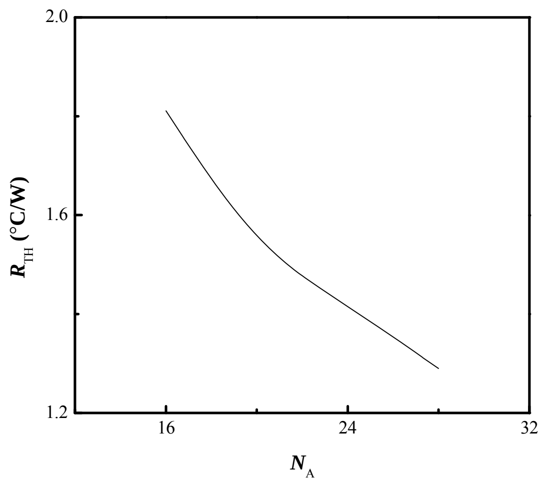

Figure 7 Effect of the number of fin arrays

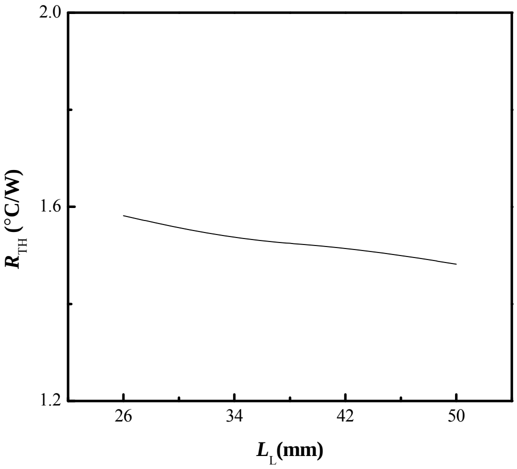

Figure 8 Effect of the long fin length

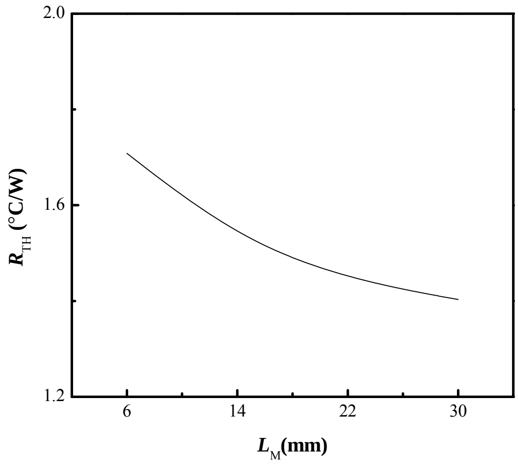

Figure 9 Effect of the middle fin length

Thus, phenomena observed in previous studies, in which the cooling performance was reduced due to the appearance of a fully developed thermal boundary layer as the number of fin arrays increased, did not occur.

Figure 8 shows the effect of the long fin length (L_L). As L_L increased, the thermal resistance showed a tendency to decrease with increasing heat transfer area. However, the improvement of cooling performance was not significant in comparison to the mass increment resulting from the increased fin length.

Figure 9 shows the effect of the middle fin length (L_M). As L_M increased, the thermal resistance decreased, at first quickly and then more gradually. This was because the thermal boundary layer of the middle fins began to overlap that of the adjacent long fins when the middle fin length exceeded 22 mm. This tendency was the same for the effect of the number of fin arrays on the cooling performance.

CONCLUSIONS

The thermo-flow characteristics of pin-fin radial heat sinks were investigated according to the fin height profile. Both natural convection and radiation heat transfer were considered. The pin-fin configuration exhibited better cooling performance due to its large heat transfer area per unit volume and repeated leading-edge effects. The thermal resistances of heat sinks with various types of pin arrays were compared to determine an appropriate reference configuration. The array with the tallest fins on the outside (Type 2) provided superior cooling performance and mass flow, and was selected as the reference. A parametric study was performed to compare the effects of various geometric parameters (outermost fin height, difference between fin heights, number of fin arrays, long fin length, and middle fin length). The effects of the outermost fin height and the number of fin arrays were found to be significant.

ACKNOWLEDGEMENT

This research was supported by Basic Science Research Program through the National Research Foundation of Korea (NRF) funded by the Ministry of Education, Science and Technology (No. 2012R1A1B3000492).

REFERENCES

[1] S.H. Yu, K.S. Lee, S.J. Yook, Natural convection around a radial heat sink, *International Journal of Heat and Mass Transfer*, Vol. 53, 2010, pp.2935~2938

[2] S.H. Yu, K.S. Lee, S.J. Yook, Optimum design of a radial heat sink under natural convection, *International Journal of Heat and Mass Transfer*, Vol. 54, 2011, pp.2499-2505

[3] S.H. Yu, D. Jang, K.S. Lee, Effect of radiation in a radial heat sink under natural convection, *International Journal of Heat and Mass Transfer*, Vol. 55, 2012, pp.505-509

[4] D.S. Jang, S.H. Yu, K.S. Lee, Multidisciplinary optimization of a pin-fin radial heat sink for LED lighting applications, *International Journal of Heat and Mass Transfer*, Vol. 55, 2012, pp.515-521

[5] Y. Yang, H. Peng, Numerical study of pin-fin heat sink with un-uniform fin height design, *International Journal of Heat and Mass Transfer*, Vol. 51, 2008, pp.4788-4796

[6] T. Bello-Ochende, J.P. Meyer, A. Bejan, Constructal multi-scale pin–fins, *International Journal of Heat and Mass Transfer*, Vol. 53 , 2010, pp.2773-2779